https://doi.org/10.21012/FC10.235443

Experimental study of a very high performance concrete slab subjected to fire on its underside and numerical modeling of the temperature field

E. OUEDRAOGO [1], S. DJAKNOUN [2], H. BENSALEM [1 2], R. BOUCHENDOUKA[2]

[1] Grenoble Alps University (UGA), Grenoble INP, Laboratory 3SR Grenoble, FRANCE
Evariste.Ouedraogo@grenoble-inp.fr

[2] H. B. University of Sciences and Technology (USTHB), Laboratory of Advanced Mechanics (LAM), Algiers, ALGERIA
sdjaknoun@usthb.dz

Abstract:

The present study deals with the numerical thermal modelling of two slab-specimens made of high performance concrete that underwent thermal spalling tests. The specimens were equipped with thermocouples located at selected points and subjected on theirs undersides to a fire of the order of Eurocode 2 ISO 834 standard fire. The thermocouples responses were recorded and reported and some of them revealed the effects of presence of water in zones near the specimens heating faces. Temperatures of the heated faces of the specimens were measured and theirs evolutions with respect to time were used as inputs of the numerical modelling. The numerical modelling of the temperature field considering the selected points and using the standard concrete thermal characteristics was not satisfactory because the discrepancies between experiment and modeling reached 41 to 63 °C at the highest temperatures. The study showed that by reducing the thermal conductivity of the concrete, it is possible to predict satisfactorily the specimen's thermal behavior during the spalling tests. Hence, the numerical modelling of spalling tests with the use of thermo-mechanical approach becomes then possible.

Key-words:

Spalling tests, High performance concrete, spalling test bench, transient nonlinear thermal, thermal numerical modelling, thermo-mechanics approach, temperature evolution prediction

1.Introduction

The study of the thermal spalling of concretes is a complex subject that has been of interest to many researchers for a long time. It has an experimental dimension of observation of the phenomenon in order to understand the leading mechanisms and to explain it. Most of the studies conducted fall under this approach [1-3]. The various studies have shown that the causes are multiple but that in summary two main causes can explain these thermal instabilities: the presence of a thermal gradient and the presence of water vapor in concrete migrating under the action of heat [4]. Studies have shown the existence of vapor pressure and thermal gradients [5]. Others focused on the influence of concrete constituents, on the differential expansion between cement paste and aggregates, on the role of water in the process of thermal instability. Although the understanding of the phenomenon is quite advanced, further studies are still needed to reinforce or refute certain assumptions currently used. It has a second dimension of modeling to help the partial understanding of observed phenomena and whose ultimate goal would be to predict these thermal instabilities. There are far fewer studies in this area [6-7]. The phenomenon is complex because it induces phenomena of heat transfer and water transfer in a complex environment where chemical reactions continue to occur. If the aim is to treat the problem as a whole, we should adopt a thermo-hydro-chemo-mechanical approach and take into account the multi-scale dimension of the problem. The more complex the approach of the problem, the better the quality of the analysis, the longer the calculations will be and the more likely are the risks of non-

convergence of the calculations. In this area, studies based on THM approaches have yielded very interesting results [Schreffler et al.].
In the present study, we have restricted the field of investigation to a thermomechanical approach which favors the effect of the thermal gradient as the main cause of the thermal spalling of concrete.
One of the difficulties of this approach, as of any other approach, lies in the correct calculation of the temperature field in the structure, a prerequisite for the thermomechanical calculation of the stresses and the damage to be realistic. To try to answer this problem, a spalling test bench was designed and realized. The first tests were carried out on specimens equipped with thermocouples which measure the temperature at certain points during the test. The proposed study investigates the extent to which the thermal behavior of the specimens can be predicted by numerical modeling of the test using the finite element method.

2.Materials and properties

The studied material is a high performance concrete which formulation is based on normalized sand. It is constituted of 0-2 mm normalized sand of the Sociéte Nouvelle du Littoral, cement CEM 1 52.5 produced by Vicat, silica fume Condensil SD95 produced by Condensil Company, superplasticizer Sika Viscocrete Tempo 10 produced by Sika and tap water. The W/C ratio is 0.25.

The various constituents of the material were mixed according to a specified protocol and cast. The molds are constituted of the assembly of Plexiglas and steel walls and measure 250x250x100 (mm). The fresh concrete was put in the molds and vibrated during 1 min 30s in two steps. In order to measure the temperature at selected points of the specimen, some thermocouples, placed along the specimen thickness, were embedded in them during the casting. Generally three thermocouples were used and located at various distances to the face of the specimen to be heated. In the first spalling test studied (Test_1) the three thermocouples were placed : first on the specimen heating face, second at 10 mm and third at 20 mm. Whereas for Test_2, the locations were : first on the specimen heating face, second at 5 mm and third at 10 mm. The thermocouples locations are displayed in Fig.1. After the vibration process, the molds are covered with a plastic film during 24 hours and then demolded. Hence, the cast specimens are squared slabs with 250 mm in length and 100 mm in thickness equipped with K type thermocouples.

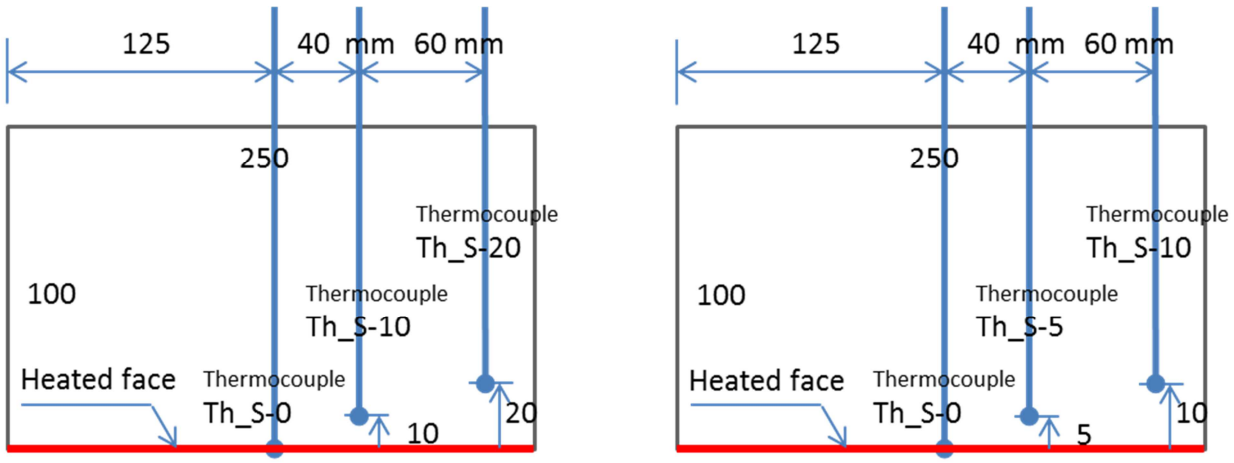

Fig.1. Sketches of the location of the measurement points for a-specimen 1 and 2- specimen 2.

In order to widely study spalling phenomenon, an original test bench was designed and fabricated. It consists of a 32 KW power burner associated with a ceramic structure forming then a sort of furnace. The burner was designed so that it heats uniformly the specimen face. The ceramic structure is constituted of vertical walls which one of them is equipped of a porthole where a camera can be placed to film the test, and an upper horizontal slab pierced with a central hole and peripheral holes. The peripheral holes are aimed at evacuating the burning gas. The central squared hole measures 245x245 in mm and faces the burner; the specimen is placed at the top of the furnace and is then heated through this hole. The burner is powered with propane gas and air and controlled by a control unit. Hence the

thermal cycle to apply to the specimen can be controlled automatically with a program or manually. At the starting of the burner, a special regime is applied during the first minute where the power is high enough in order to check the good working of the apparatus and then it decreases down to a minimum value at which the spalling test can begin. The control unit is connected to two thermocouples placed in the furnace aimed at insuring the thermal regulation: regulation and security thermocouples. Another independent type K thermocouple is also placed in the furnace beside the regulation thermocouple in order to measure the temperature in the furnace.
During the spalling test, the three embedded thermocouples and the independent thermocouple placed in the furnace are connected to an independent data acquisition system that acquires the data all along the spalling tests. The test bench is under development and other sensors are planned to be used later, especially acoustic and pressure sensors. The global view of the apparatus is displayed in Fig.2.

a

b

Fig.2. Photo of a- a global view of the spalling test bench and b- a detailed view of the specimen equipped with the three thermocouples.

3.Experimental study

The test consisted in placing the instrumented test specimen on the furnace once the burner reached it minimum power after the starting regime and in beginning the data acquisition. During the tests presented here, the burner power was increased manually in order to estimate the heating rate close to the ISO 834 standard curve. The evolutions of the various acquired temperatures with respect to time were visible in real time thanks to data acquisition software. Occurring events such as noise or explosion are collected during the test. Some photos of water coming out of the lateral or upper faces of the specimen were taken and dated. The thermocouples responses gave interesting information on what happened during the test. Two tests that differ from the embedded thermocouples locations and the heating rate are presented in this study. In the two cases, thermal spalling occurred during the tests.
In Fig.3 are displayed the response of the thermocouple located in the furnace (TH_Furn), the responses of those embedded in the specimen at various distances to the heated face (Th_S0, TH_S10, TH_20) and the fire standard ISO 834 curve of Eurocode 2 (TH_ISO834). Globally, the responses of all the thermocouples increased with increasing time. The study concerned the ten first min of the spalling test (600 s). The evolution with respect to time of TH_Furn is higher at any time than the curve Th_ISO834 indicating then that the applied power cycle was more severe than the recommended standards. It also presents sudden increase (at time 75 and 310 s) corresponding to the sudden increase of the power that was controlled manually. The evolution of the temperature of the thermocouple which tip was located in the burned face is quite different in intensity from the temperature in the furnace but present the same discontinuities. The difference of intensity is due to the influence of the thermal inertia of the concrete surrounding the thermocouple. The sudden decrease of the temperature observed at time 487s was the consequence of the occurrence of thermal spalling that was noisy. The TH_Furn temperature decreased from 857 to 737 °C whereas the one of TH_S0 decreased from 424 to

358 °C. That was not the first time that the thermal spalling occurs in the specimen but it was the first time it impacts visibly the thermocouples responses. We think that the temperature sudden decrease is due to a reduction of burner power consequence the projection of concrete splinters on it. But the zone surrounding the TH_S0 was not affected by the spalling and that's why its temperature decreased. Temperature of the thermocouple located at 10 mm from the heated face (TH_S10) increased regularly with increasing temperature and seemed not affected by the effects of power sudden increases as the previous ones but was slightly affected by the power sudden decrease. The thermocouple located at 20 mm (TH_S20) behaved as the previous one but at lower temperatures logically. But surprisingly at time 487s, the temperature slightly increased instead of decreasing as previously. We are still looking for explanations.

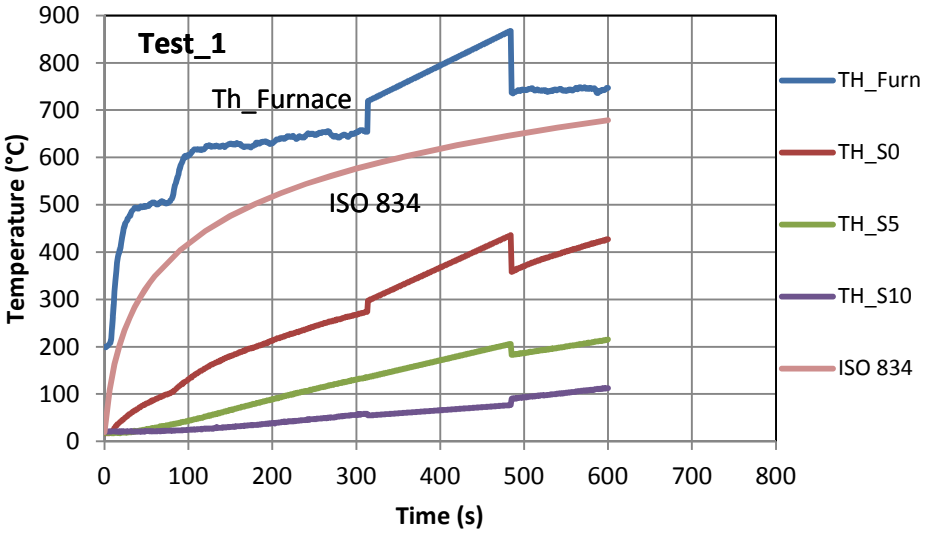

Fig.3. Temperature evolution with respect to time in specimen 1.

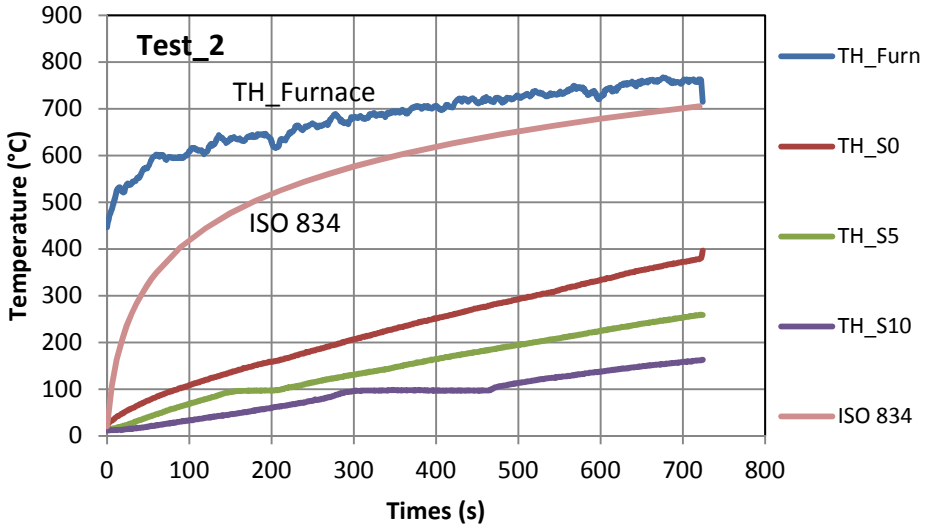

Fig.4.Temperature evolution with respect to time in specimen at a point located in the heated face and at 10 and 20 mm to the heated face, respectively.

Fig.4 display results of Test_2 (specimen 2). As the previous test, the furnace temperature (TH_Furn) was higher than the standard ISO834 fire curve (TH_ISO834) and then the test was more severe than the recommendations. The furnace temperature evolve regularly because however the power regulation remained manual, the increase stepping was reduced. Until time 720 s, no sudden variation of the temperature was observed. The temperature of the thermocouple located in the heated face (TH_S0) increased regularly and quasi-linearly with respect to time. Temperatures of thermocouples

located at 5 mm (Th_S5) and 10 mm (TH_10) from the heated face evolve quasi linearly with respect to time during the test but with a special local evolution. The Th_S5 curve presents a stage at about 100°C between time 150 and 205 whereas TH_S10 presents a stage at the same temperature between time 300 and time 468 s. These observations are very interesting. The first observation is that 100°C is the boiling temperature of water. That mean that at time 150 a front of liquid water reached the thermocouple located at 5 mm from the heated face. The duration of the stage is the time necessary for the water to totally vaporize condition necessary for the temperature to increase. At time 205 s the water was totally vaporized. The water front went deeper and at time 300 s it reached the location of thermocouple TH_S10 (10 mm from the heated face) and the front contained more water. That's why more time was necessary to the water to vaporize at this location, 168 s instead of 55 s previously. This last test evidence the presence of water and its movement in the material induced by the heating of the specimen face. One can image the formation of the famous water clog. The consequence is that presence of water in the concrete probably affects the heat transfer in the material. When using THM modelling approach, one could probably modelled and predict exactly the temperature increase during the test. But thermo-mechanical approach doesn't take into account constitutively the presence of water in the material and who influences its behavior. The aim of the study is to find which material thermal characteristic can help in predicting globally the thermocouples responses.

4.Numerical study

The aim of the study now is to model the thermal behavior the slabs specimen during the spalling tests reported previously. The specimen is has a parallelepipedal shape with the width equal to the length and is uniformly burned on one of its large face. A 3D modelling is a priori convenient. Thanks to the two present symmetry planes and the uniformity of the loading, the study of a fourth of the specimen is representative of the whole specimen. We will retain one fourth of the specimen to define the element finite model. Hence this model had six faces where some thermal conditions were applied: the upper face that is heated, the lower face in contact with the air, the two symmetry faces where symmetry conditions should be applied and two remaining free faces in contact with the air.
The burner heated the specimen at its face and the mode of heat transfer inside the specimen is the conduction governed by Fourier heat equation. This equation can be established from the first principle of thermodynamics and its general form is as following:

$$div\left(\alpha\overrightarrow{gradT}\right) - \rho C_p\left(\frac{\partial T}{\partial t}\right) = -P \quad (1)$$

Where ρ is the material density, α is the material conductivity, C_P the material specific mass and P the calorific power of the internal sources. In the case where the thermos-physical characteristics of the material depend on the temperature, it takes the following form:

$$\alpha(T)\Delta T + \frac{d\alpha}{dT}\left(\overrightarrow{gradT}\right)^2 - \rho(T)C_p(T)\left(\frac{\partial T}{\partial t}\right) = -P \quad (2)$$

These last equations were used in the present study since the temperature field varied between 20 and 500°C a range where the thermo-physical characteristics varied significantly. No interne sources were present so P equaled 0.
The temperature field at any point of the studied domain characterized by its geometrical coordinates x depend on time and can be written T(x,t).
The initial conditions were imposed at any point of the studied domain characterized were:

$$T(x,0) = T_i \quad (3)$$

where T_i is the initial temperature, generally set at 20°C.

Boundary conditions are defined on the various faces of the model. First the large free face (A1 in Fig.5) and the lateral free faces (A3 and A6 in Fig.5) of the specimen in contact with air were subjected to convection governed by the following equation:

$$\varphi = H_v(T(M_i,t) - T_{ext}) \quad (4)$$

Where φ is the exchange flux density, H_v is the heat exchange coefficient, $T(M_i,t)$ is the temperature at any point M_i of the considered surfaces and T_{ext} is ambient temperature generally set to 20°C. As the

other thermo-physical characteristics, H_v a priori depends on temperature and this should be encountered.
As to the two symmetry faces of the finite model (A4 and A5 in Fig.5), they are not subjected to any exchange and are characterized by adiabatic conditions (no heat transfer).
Lastly the second large face (A2 in Fig.5) of the finite element model is the loading face and was subjected to a temperature-imposed loading. The formulation defining the loading condition is:

$$T(M_i, t) = TH\_S0(t) \quad (5)$$

Where TH_S0 is the temperature measured by the thermocouple located at the burned face during the spalling test. The temperature-imposed condition was applied to the upper face in thermal modelling in order to obtain a better view when displaying the temperature field in the specimen, contrary to the experience where the lower face was heated.
The material thermo-physical characteristic and their evolution with respect to temperature were taken from the Eurocode 2: between 20 and 800°C, the density decreased from 2300 to 2185 $kg.m^{-3}$, the specific mass increased from 900 to 1100 $J.kg^{-1}.K^{-1}$ and the thermal conductivity of the material decreased from 1.95 to 0,724 $Wm^{-1}K^{-1}$, respectively. During this study, the thermal exchange coefficient H_v was kept constant at 20 $W.m^{-2}.K^{-1}$.

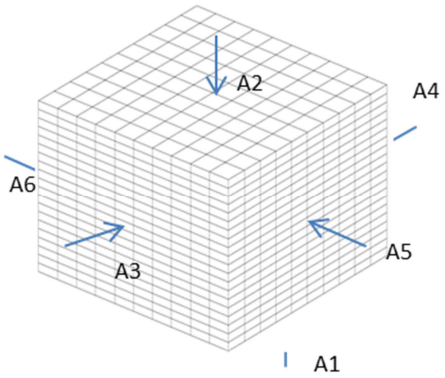

Fig.5. Definition of the areas where boundary conditions are applied.

The finite element code CAST3M developed by CEA-SACLAY in France was used for the transient nonlinear thermal modelling of the tests. Cubic quadratic 3D finite elements (CU20) were used to mesh the model. The reduced finite element model was discretized by 10 divisions in the length and the width and 20 divisions in the height. This generated element size of 12.5 mm in length and width and 5 mm in height. Some calculations that were undertaken showed that reducing the length and width finite elements size doesn't affect significantly the thermal behavior but affect considerably the computing time. That's why the current mesh was used. This mesh was designed so that any location of the thermocouples in the specimen matches with a node of the mesh. Hence the comparison of numerical and experimental results will be done on the base of coincident geometric points. Hence along the specimen height, a node is present every 5 mm.
In the present study temperature imposed thermal loading was adopted since experimental investigations allowed the measurement of the heated face of the specimen. The evolution of the heating face measured by thermocouple TH_S0 will be the imposed temperature during the modelling. That was one of the goal of the design and fabrication of the test bench.

5.Results and discussion

The comments of the experimental results were made previously in section 3 and the following results and discussion will just concern modelling and its ability to predict the material thermal behavior characterized by experimental measurements. In Fig.6 is displayed the temperature field in the specimen 1 obtained at time 470 s. It can be seen that the temperature vary essentially with the thickness of the specimen.

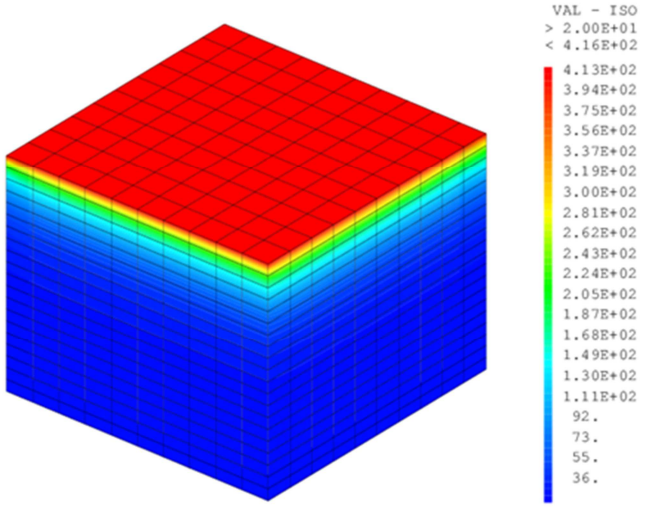

Fig.6. Temperature distribution in the specimen at time 570 s for specimen 1.

5.1.Modelling with standard values of the thermo-physical parameters

Fig.7 displays experimental curves and thermal modelling curves with standard evolution of the material thermal characteristics, which mean according to Eurocode 2. The thermal modelling curves are named M_HF-XX where XX is the distance of the considered node to the heated face of the specimen. Hence a modelling curve M_HF-XX is to be compared to the experimental curve TH_SXX. First of all it can be noticed that the modelling M_HF curve is strictly superimposed with the TH_S0 curve as expected. That is the proof that the temperature-imposed condition is well accounted for during the calculations. At a node located at 10 mm inside the specimen the modelling curve matches the experiment Th_S10 curve at low temperatures and but with increasing temperature the discrepancy (M_HF_XX-TH_SXX) is positive and tends to increase. To evaluate these discrepancies, three reference temperatures were adopted: 200, 300 and 400°C. Considering Fig.7 the temperature discrepancies were: 10, 16 and 41°C at times 200, 400 and 600 s, respectively. In our opinion, these discrepancies are significant. Considering nodes located at 20 mm from the heated face the measured discrepancies between M_HF-20 and TH_S20 were of the same order as previously: 10, 36 and 45°C at the same times. Hence, the thermal modelling of the specimen behavior with the standard thermo-physical characteristics is not really satisfactory because the discrepancies are too high.
The results of Test_2 corresponding to specimen 2 are displayed in Fig.8. The same analysis as at the same temperatures references as undertaken previously was applied to the results of Test_2 and gave amplified results. Of course experimental Th_S0 and modeling M_HF curves are superimposed as expected. As previously, numerical modeling clearly overestimates the specimen temperature inside the specimen. Hence, at a node located at 5 mm from the heated face, the measured discrepancies were: 17, 24 and 32°C at times 200, 400 and 600 s, respectively. And at a node located at 10 mm from the heated face the temperature discrepancies increased to 20, 45 and 63°C at the same times. In this second Test, the discrepancy between modeling experiment increased quasi monotonically with increasing temperature. As for the previous specimen, the thermal prediction of the specimen thermal behavior through numerical modeling is not satisfactory. Criteria should be defined in order to define what maximum value of the discrepancy would be satisfactory. In our opinion, a maximum discrepancy absolute value of 10°C all along the curve would be considered satisfactory.

5.2.Modelling with modified conductivity

Examining the thermal equations used to compute the specimen's thermal fields, it appears that 4 parameters can potentially be adjusted, in an approach of inversed problem, in order to improve the modelling prediction. The first one is the power exchange parameter H_v expressed in (Eq. 5) and is relative to the boundary conditions. The other three ones are relative to the material thermo-physical

parameters expressed in (Eq. 2) C_p, α and ρ. In the present study, only the power exchange parameter H_v and the material thermal conductivity were encountered.

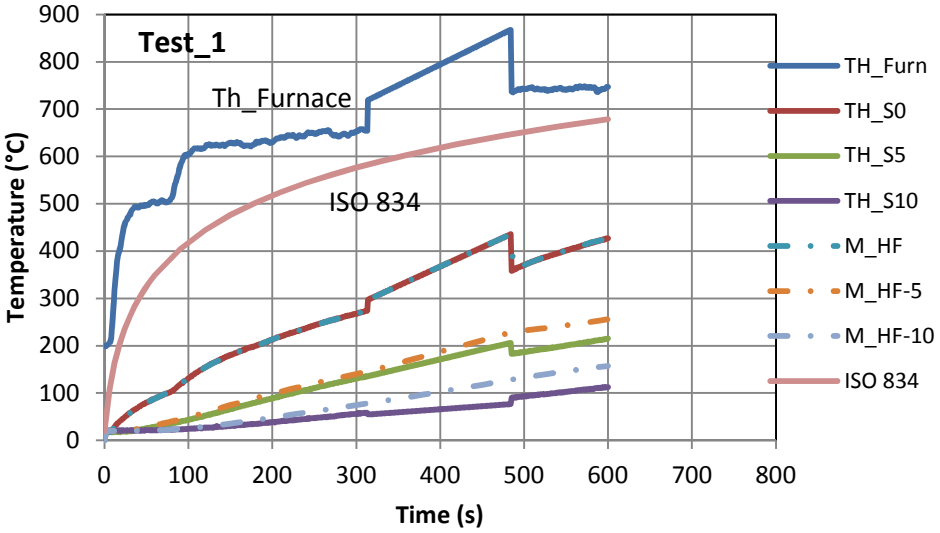

Fig.7. Comparison of the modeling results of specimen 1 thermal behavior considering initial conductivity curve with experimental results. The modeling could be improved.

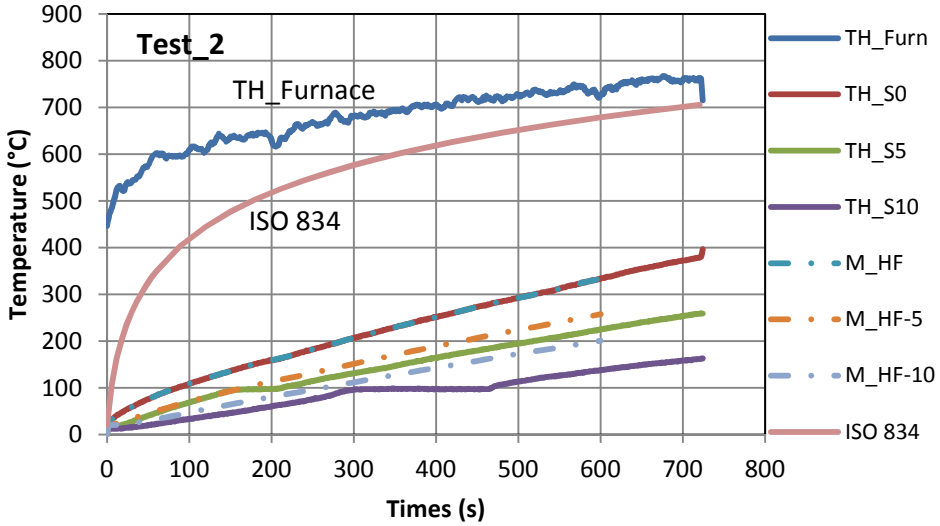

Fig.8. Comparison of modeling results of specimen 2 thermal behavior considering initial conductivity curve with experimental results. The modeling could be improved.

The first sensibility study concerned the power exchange parameter. Calculations were run with H_v values ranging from 6 to 50 $Wm^{-2}K^{-1}$. The changes observed affected the temperature of the very peripheral point very near the faces under convection and the variation was very weak. The huge majority of the specimen was not affected at all. The temperature curves at the selected nodes were rigorously the same as the standard value. Power exchange parameter was not the relevant parameter. If any, the solution was to find among the material thermal characteristics. The analysis of the thermal curves where modelled ones seemed to overestimate the experiment ones suggest us the idea of reducing the value of the material thermal conductivity. Indeed, the presence of water delays the heat transfer in the specimen and acts as if the material conductivity was reduced. The thermal conductivity evolution with respect to temperature was then reduced of an increasing $\Delta\lambda$ all along the temperature dependence curve until the modelled curves fit with the experimental ones. At high temperature the value of $\Delta\lambda$ decreased so that the thermal conductivity remain positive and keep reasonable values at 800°C. The standard and modified conductivity curves are displayed in Fig.9. This figure displays

three curves: the standard curve and the optimum curves found for specimens 1 and 2, respectively. The optimum curves are named K_-XX in Fig.9 where XX is the $\Delta\lambda$ value applied at 20°C. Hence, XX equals 0.6 and 0.9 for specimen 1 and 2, respectively.

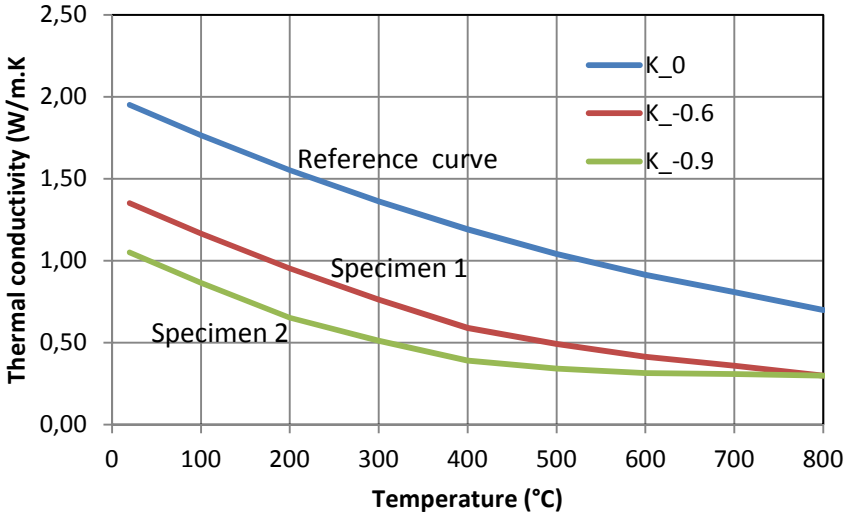

Fig.9. Evolution of the initial and the modified thermal conductivities with respect to temperature.

By reducing the thermal conductivity value, it was possible to obtain the results displayed in Fig. 10 and 11 for specimen1 and specimen 2, respectively. In Fig.10 the modelled curves M_HF-XX are quasi superimposed with the experimental ones TH_SXX. The discrepancies observed at the node located at 10 mm to the heated face at times 200, 440 and 600 were: -6, -15 and -1.5 °C. At the node located at 20 mm to the heated face, at the same times the discrepancies were: -1.7, 11 and 4 °C. The results of the calculations are quite satisfactory. As in Fig.10, in Fig.11 the modelled curves M_HF-XX are quasi superimposed with the experimental ones TH_SXX. The discrepancies observed at the node located at 5 mm to the heated face at times 200, 440 and 600 were: -0.2, -3 and -6 °C. At the node located at 10 mm to the heated face, at the same times the discrepancies were: 3, 11 and 15 °C. The results of the calculations are quite satisfactory.

In order to obtain such satisfactory results, it was necessary to reduce the thermal conductivity of the material at an important value of 30% in the case of specimen 1 at a very important value of 45% in the case of specimen 2. Such a reduction value may exceed the uncertainties on the value of the thermal conductivity of concrete accounting for the variety of concrete and then may not be realistic. But the idea in this study is to determine an equivalent thermal conductivity of the studied material in which several mechanisms that cannot be modelled by the thermomechanical (TM) approach take place. This paper show that such a solution seems possible.

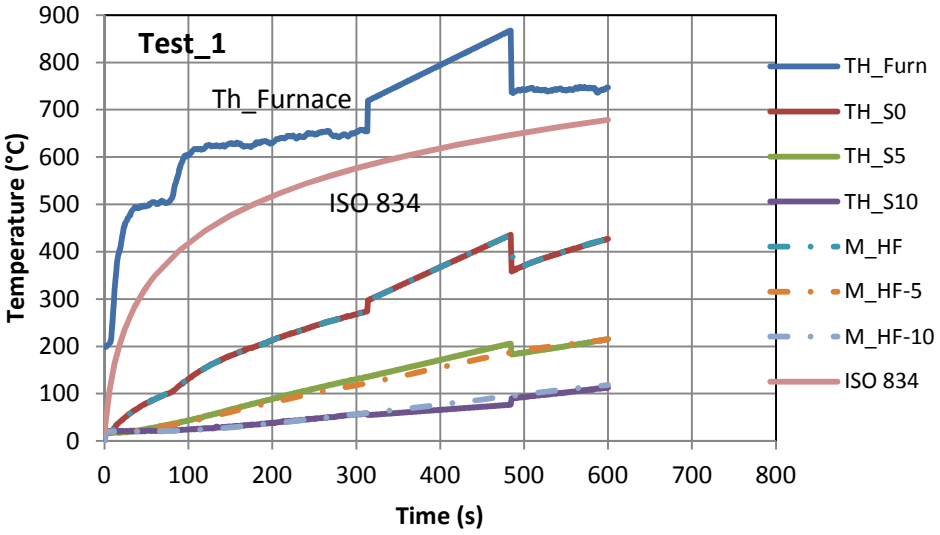

Fig.10. Comparison of the results of modeling of the thermal behavior of specimen 1 considering the modified conductivity curve with experimental results. The modeling was satisfactorily improved.

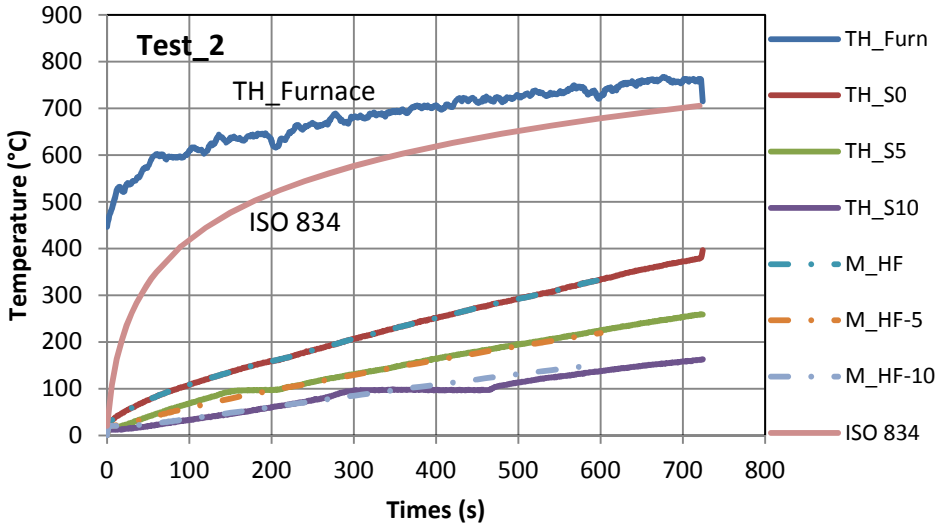

Fig.11. Comparison of the results of modeling of the thermal behavior of specimen 2 considering the modified conductivity curve with experimental results. The modeling was satisfactorily improved.

Conclusion

Two slab-specimens of high performance concrete based on 0-2 mm normalized sand were subjected to spalling tests consisting in heating theirs underside faces with fire of the order of the ISO 834 standard fire. The specimens were equipped with thermocouples that measured continuously the temperature in three points during the spalling tests. The studied material underwent spalling during the tests. A numerical modeling was undertaken to predict the temperature measured by the embedded thermocouples and the following conclusions can be drawn:

-The domain of interest in the first 10 to 12 min after the beginning of heating the specimens. During the thermal spalling tests, spalling occurred in the two specimens and the responses of the thermocouples located in the heated face of the specimens varied witnessing of these instabilities. The recording of the temperature with respect to time of two of the thermocouples of specimen 2 showed temperature stages at 100°C, probable consequence of presence of water or move of water front.

-The numerical thermal calculations were undertaken in nonlinear transient thermal thanks to the CEA-Saclay CAST3M finite elements code. The concrete thermo-physical characteristics standard

curves given by the Eurocode 2 were first used. The results of modeling were not satisfactory for specimen 1 or for specimen 2. Discrepancies up to 45 °C were observed.
- Modeling the thermal behavior of concrete with thermo-mechanical approach is restrictive so that to predict the temperature field some of the thermal characteristics may be adjusted slightly or strongly. By reducing the material thermal conductivity of 0.6 for specimen 1 and 0.9 for specimen 2, it was then possible to numerically model satisfactorily the evolution of the temperature at the selected nodes. Discrepancies were about 5°C with exceptional values at 15°C.

References

[1] G.A. Khoury and B. Willoughby. Polypropylene fibres in heated concrete. part 1 : molecular structure and materials behaviour. Magazine of concrete research, 60(2) :125– 136, 2008.
[2]P. Kalifa, G. Chéné, and C. Gallé. High temperature behaviour of hpc with poly propylene fibres : from spalling to microstructure. Cement and Concrete Research, 31(10) :1487–1499, 2001.
[3] C. G. Han, M. C. Han, and Y. S. Heo. Spalling properties of high strength concrete mixed with various mineral admixtures subjected to fire. Concrete Structures and Materials, 2(1) :41–48, 2008.
[4] G.A. Khoury. Polypropylene fibres in heated concrete. part 2 : pressure relief mechanisms and modelling criteria. Magazine of concrete research, 60(3) :189–204, 2008.
[5] P. Kalifa, F.D. Menneteau, and D. Quenard. Spalling and pore pressure in hpc at high temperatures. Cement and Concrete Research, 30 :1–13, 2000.
[6] J. Ožbolt, G. Periškić, M. Jelčic, and H.W. Reinhardt. Modelling of concrete exposed to high temperature. In 1st International Workshop on concrete spalling due to Fire Exposure, pages 461–469, Leipzig, 2009.
[7] Ozbolt J et al. 3D numerical analysis of reinforced concrete beams exposed to elevated temperature. Eng Struct (2013) http://dx.doi.org/10.1016/j.engstruct.2012.11.030